AUTONOMOUS TECHNOLOGIES CORPORATION

(2)

MULTI-DIMENSIONAL LADAR TRACKING AND ADAPTIVE GRASPING FOR SPACEBORNE ASSEMBLY OF SDI PLATFORMS

Contract No. DASG60-89-C-0079

Effective: 1 June 1989
Expiration: 1 December 1989

SBIR Phase I Final Report

A002

Reporting Period 1 June 1989 to 31 November 1989

Sponsored By:

SDIO Innovative Science and Technology Office

Managed By:

U. S. Army Strategic Defense Command

Submitted By:

Randy W. Frey
Autonomous Technologies Corporation
Orlando, Florida

The views and conclusions contained in this document are those of the authors and should not be interpreted as necessarily representing the official policies, either expressed or implied, of the Government.

520 N. Semoran Blvd., Suite 180 • Orlando, FL 32807
(407) 282-1262

Unclassified

SECURITY CLASSIFICATION OF THIS PAGE

REPORT DOCUMENTATION PAGE

Form Approved OMB No. 0704-0188

1a. REPORT SECURITY CLASSIFICATION: Unclassified

1b. RESTRICTIVE MARKINGS: None

2a. SECURITY CLASSIFICATION AUTHORITY: N/A

2b. DECLASSIFICATION / DOWNGRADING SCHEDULE: N/A

3. DISTRIBUTION / AVAILABILITY OF REPORT: Unlimited

4. PERFORMING ORGANIZATION REPORT NUMBER(S): N/A

5. MONITORING ORGANIZATION REPORT NUMBER(S): DI-MISC-80048,A002

6a. NAME OF PERFORMING ORGANIZATION: Autonomous Technologies Corp.

6b. OFFICE SYMBOL *(If applicable)*: N/A

7a. NAME OF MONITORING ORGANIZATION: U.S. Army Strategic Defense Command

6c. ADDRESS *(City, State, and ZIP Code)*:
520 N. Semoran Blvd., Suite 180
Orlando, Fl. 32807

7b. ADDRESS *(City, State, and ZIP Code)*:
P.O. Box 1500
Huntsville, Al. 35807-3801

8a. NAME OF FUNDING / SPONSORING ORGANIZATION: SDIO Innovative Science and Technology Office

8b. OFFICE SYMBOL *(If applicable)*: N/A

9. PROCUREMENT INSTRUMENT IDENTIFICATION NUMBER: DASG60-89-C-0079

8c. ADDRESS *(City, State, and ZIP Code)*:
Pentagon
Washington, D.C. 20301-7100

10. SOURCE OF FUNDING NUMBERS

PROGRAM ELEMENT NO.	PROJECT NO.	TASK NO.	WORK UNIT ACCESSION NO.
P63222C	N/A	N/A	N/A

11. TITLE *(Include Security Classification)*: Multi-Dimensional LADAR Tracking and Adaptive Grasping for Spaceborne Assembly of SDI Platforms (Final Report)

12. PERSONAL AUTHOR(S): John A. Bohlin, Randy W. Frey

13a. TYPE OF REPORT: Final Report

13b. TIME COVERED: FROM 6-1-89 TO 11-31-89

14. DATE OF REPORT *(Year, Month, Day)*: 1990 February 16

15. PAGE COUNT: 37

16. SUPPLEMENTARY NOTATION: N/A

17. COSATI CODES

FIELD	GROUP	SUB-GROUP
N/A	N/A	N/A

18. SUBJECT TERMS *(Continue on reverse if necessary and identify by block number)*: Adaptive, Grasping, LADAR, CAD, Database, Tracking, Recognition.

19. ABSTRACT *(Continue on reverse if necessary and identify by block number)*

The most successful approaches to both machine target recognition and robot arm manipulation have been those where tasks are completely pre-specified. In such systems there is little room for deviations inrobot path motion or target location and orientation. A novel approach to robotic implementation such as spaceborne assembly of SDI platforms are too difficult for existing robots because random occurrences and large numbers of external variables preclude the complete specification of tasks off-line. The proposed system has strong adaptability due to the following innovations: Registered video and range laser radar sensign (i.e., a one-to-one correspondence between visual and range data). This allows fast, accurate 3D target recognition as part of an autonomous CAD model based recognition system for Phase II, or as input to teleoperator control in Phase I. Closed loop range and video feed back for grasper guidance using the pose matching concept where target and grasper are both in the field of view, and CAD derived track points are used for position and orientation error signals. Adaptive control systems, Manipulators, Computer aided design, Computer vision, Robotics, Lasers, Optical radar tracking.

20. DISTRIBUTION / AVAILABILITY OF ABSTRACT: ☒ UNCLASSIFIED/UNLIMITED ☐ SAME AS RPT. ☐ DTIC USERS

21. ABSTRACT SECURITY CLASSIFICATION: Unclassified (EDC)

22a. NAME OF RESPONSIBLE INDIVIDUAL: John C. Johnson

22b. TELEPHONE *(Include Area Code)*: 205-895-4394

22c. OFFICE SYMBOL: CSSD-H-V

DD Form 1473, JUN 86 *Previous editions are obsolete.*

SECURITY CLASSIFICATION OF THIS PAGE

Unclassified

TABLE OF CONTENTS PAGE

I. EXECUTIVE SUMMARY

Under the DoD/SDI SBIR Phase I Program entitled "Multi-Dimensional LADAR Tracking and Adaptive Grasping for Spaceborne Assembly of SDI Platforms", Autonomous Technologies Corporation was contracted to demonstrate the innovative concepts of integrating a co-boresighted visible video intensity channel to our existing programmable fovea with peripheral vision LADAR and developing reference data generated by a CAD database to be utilized with the new registered video data to derive robotic grasper commands via the "pose matching" concept. To accomplish this the project was broken down to four primary tasks which were modifying the existing ATC LADAR for registered range and visible video, creating the "pose matching" software, creating a non real time breadboard robotic demonstration to test the basic innovative concepts and, developing a Phase II concept definition.

It is with pleasure that we report the successful implementation and demonstration of the task put before us. The first of these was the modification of our resident LADAR to include a registered visible channel. This was accomplished by modifying our opto-mechanical assembly to include a dichroic beamsplitter for visible and 10.6 μm duplexing. Additionally, detector circuitry was built and implemented successfully. One minor problem encountered in the visible channel was the presence of 60 Hz indoor lighting noise. This is not a limiting issue because 60 Hz lighting noise is not present in the spaceborne solar illumination case and our Phase II vision processor implementation will remove periodic noise quite easily. The second task of the program was to develop the "pose matching" software to aid in the robotic grasping. The software consists of 2 algorithms coded in the C programming language. The first was the vector points algorithm, which takes as input registered range and orientation data from the target and the robotic end effector, producing as output motion commands instructing the robot to move into position and grasp the target. This algorithm was successfully demonstrated using the Phase I robot and LADAR hardware. The second part of the software was the generation of correlations between generated reference images and actual range images. This algorithm offers the widest range of application and is the focus of our Phase II project.

The third portion of the project was the robot demonstration. To test our concept ATC subcontracted to Honeybee Robotics for robot systems analysis and for the loan of a GMF S-100 six axis industrial robot with a parallel gripper end effector. Early systems analysis performed by ATC and Honeybee indicated that an industrial grade (GMF S-100) robot would need to be used instead of a "toy" robot, as originally proposed. The analysis showed that a "toy" robot did not possess the precision nor coordinate system transformation capabilities required to perform the tasks at hand. Therefore, the GMF S-100 industrial robot was used. Installing the GMF robot required extensive hardware integration such as adding new lab space, installing 3-phase electrical power, building an interface from the robot to the RS232 port on the controlling computer. As well, software had to be generated to control the robot via its KAREL Operating System. World, user, and tool coordinate systems had to be derived as well as defining the relative and absolute position and movement controls. All in all, the demonstration went very well and the concepts were successfully demonstrated with only minor problems arising. One such problem was inability of the sensor to generate adequate range images on diffuse targets . This was due to the specific implementation of a quick look range processor with 300 MHz IF bandwidth compared to the 40 to 60 dB improvement in our Phase II LADAR FFT based range processor. Despite this, high accuracy range data on miniature, homemade solder retro-reflects was sufficient for the robotic grasp algorithm.

The fourth and final task of this program was the conception of a Phase II program approach. Several trips were made to gather technical data from SDIO and NASA/JSC. The concept definition as defined in our Phase II proposal includes contributions from our key consultants in the areas of computer architecture, Fourier Domain processing, geometric data processing, and hardware/software implementation. As our Phase II approach, we proposed a joint SDI/NASA cooperative effort to ensure a high payoff. We proposed to develop the end-to-end LADAR Vision Processor under the SDI Phase II program and combine it with the NASA

Phase II LADAR sensor program already under development. This promises to have high payoff for Autonomous Satellite Servicing if the joint Phase II projects are successful.

Although minor problems were encountered, this programs' innovative concepts were demonstrated and the technical issues uncovered provide an excellent opportunity for future investigation.

II. REGISTERED VISIBLE VIDEO CHANNEL IMPLEMENTATION

The first task performed in this program was the modification of the existing ATC LADAR to incorporate the visible video channel. This was accomplished by inserting a dichroic beamsplitter in the optical return path of the opto-mechanical assembly. The beamsplitter is a ZnSe substrate 0.5" in diameter and 2 mm thick with the side 1 coated for maximum transmission at 10.6 μm and maximum reflectance from 0.5 μ to 1.0 μ, at a 45 degree angle of incidence. Side 2 of the beamsplitter is AR coated for 10.6 μm. Figures 1 and 2 show the 10.6 μm transmittance and 0.5 μm - 1.0 μm reflectance curves, respectively, of the beamsplitter used, tested at 0 degrees angle of incidence. Once the visible portion of the received signal is broken out, it is focussed by an 88 mm focal length lens onto the visible detector. This focal length lens was chosen to match the Fields of View of the IR and visible returns.

$$\Theta \text{ vis} = d/f = .5 \text{ mm}/88 \text{ mm} = 5.7 \text{ mr}$$

$$\Theta_{IR} = (4 * \text{lambda})/(\text{pi} * D) = (4 * 10.6 \times 10^6)/(3.14 * 2.5 \text{ mm}) = 5.4 \text{ mr}$$

The returns need to be closely matched in FOV so that images taken simultaneously in the IR and visible will be registered with respect to each other. Once the visible return is focussed onto the detector, the signal is amplified and filtered and is fed into the transputer data acquisition portion of the ATC LADAR. The visible detector and amplifier circuit is shown in Figure 3. Several images were taken using the visible video channel with several varieties of targets.

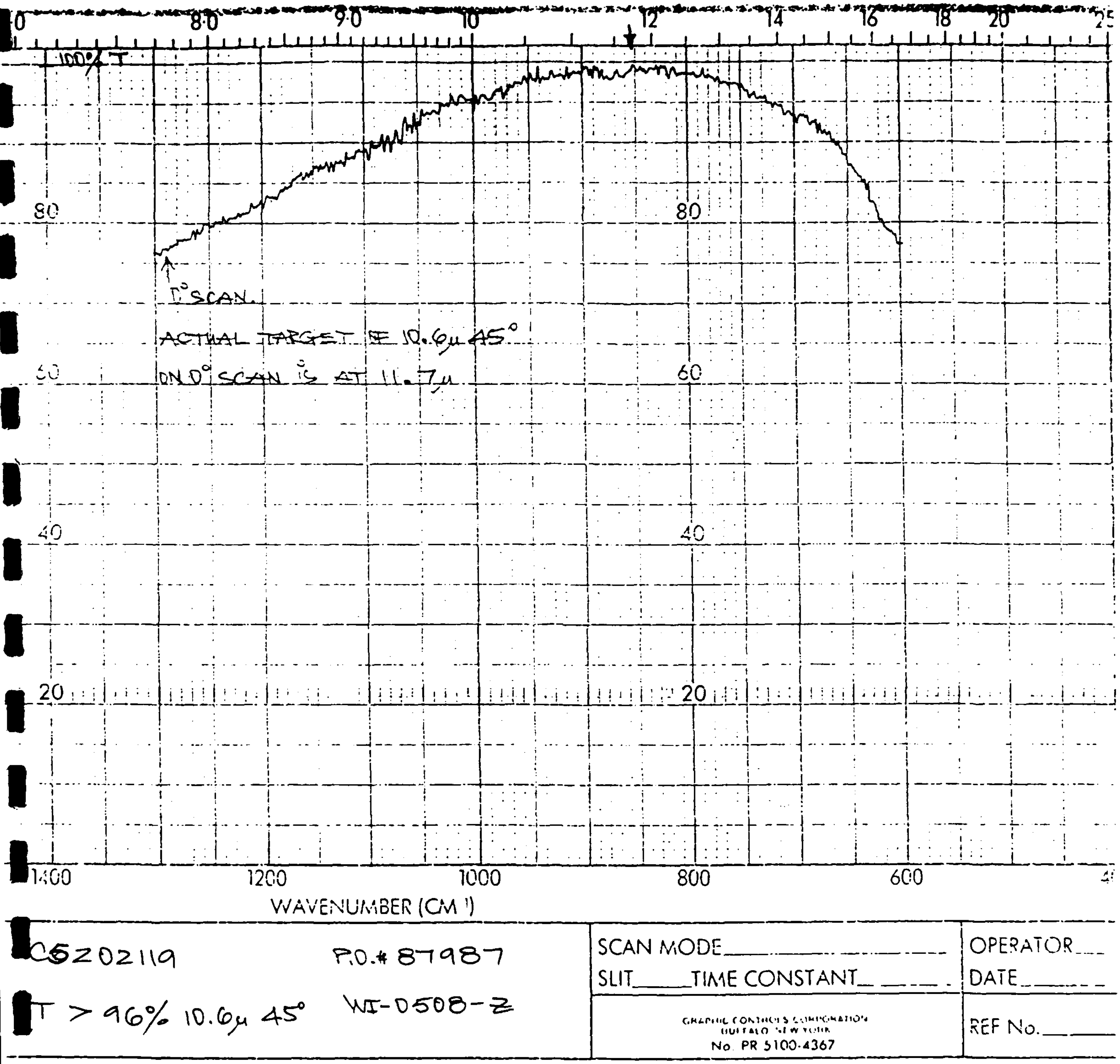

Rocky Mountain Instrument Co.
1501 South Sunset St.
Longmont, CO 80501

Figure 1

NO. PR 80 119849

PRINTED IN U.S.A.

Rocky Mountain Instrument Co.
1501 South Sunset St.
Longmont, CO 80501

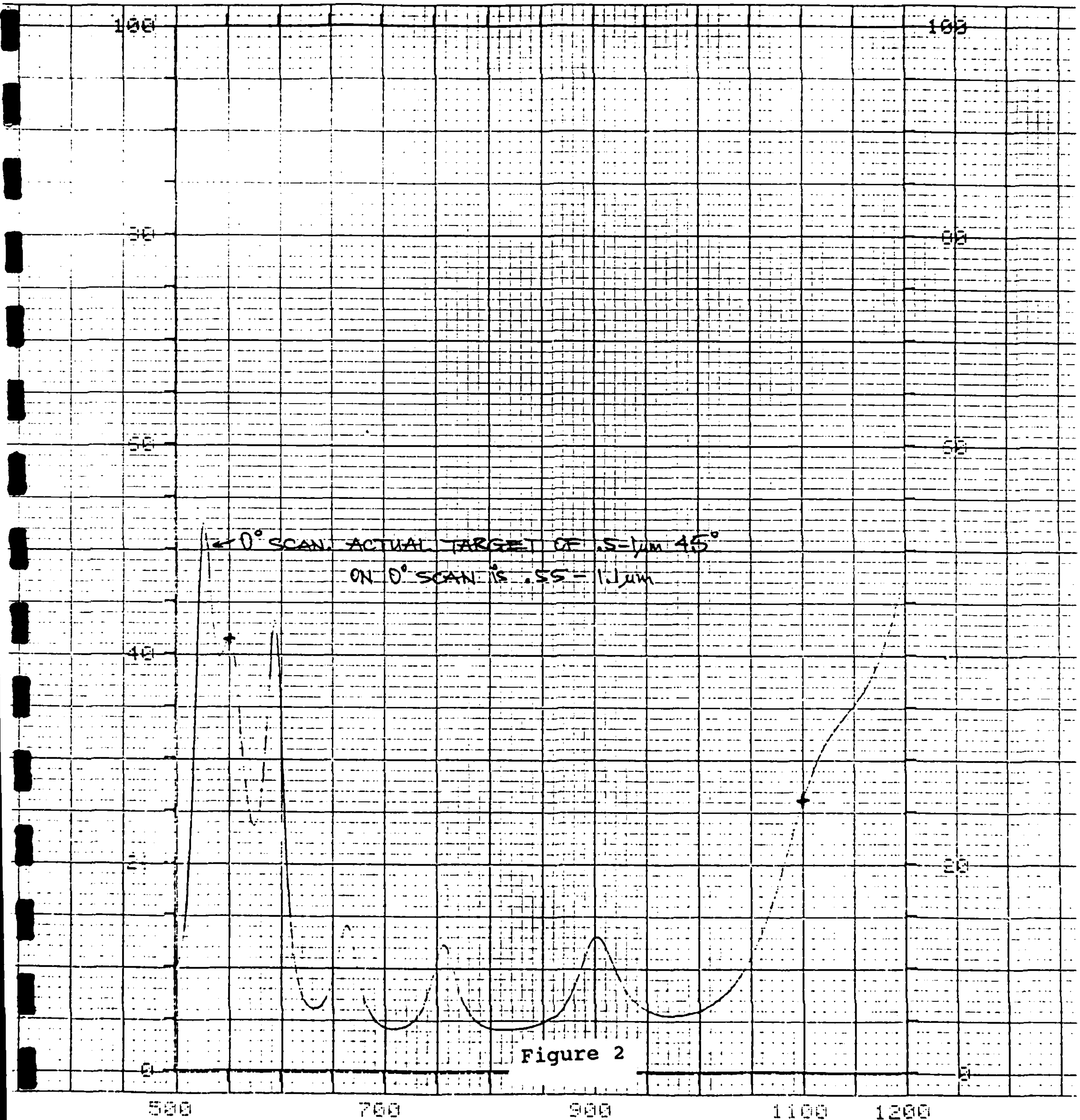

Figure 2

R ave. >80% 0.5-1µm 45° P.O.#87987

CS202119 WI-0508-Z

VISIBLE DETECTOR SCHEMATIC

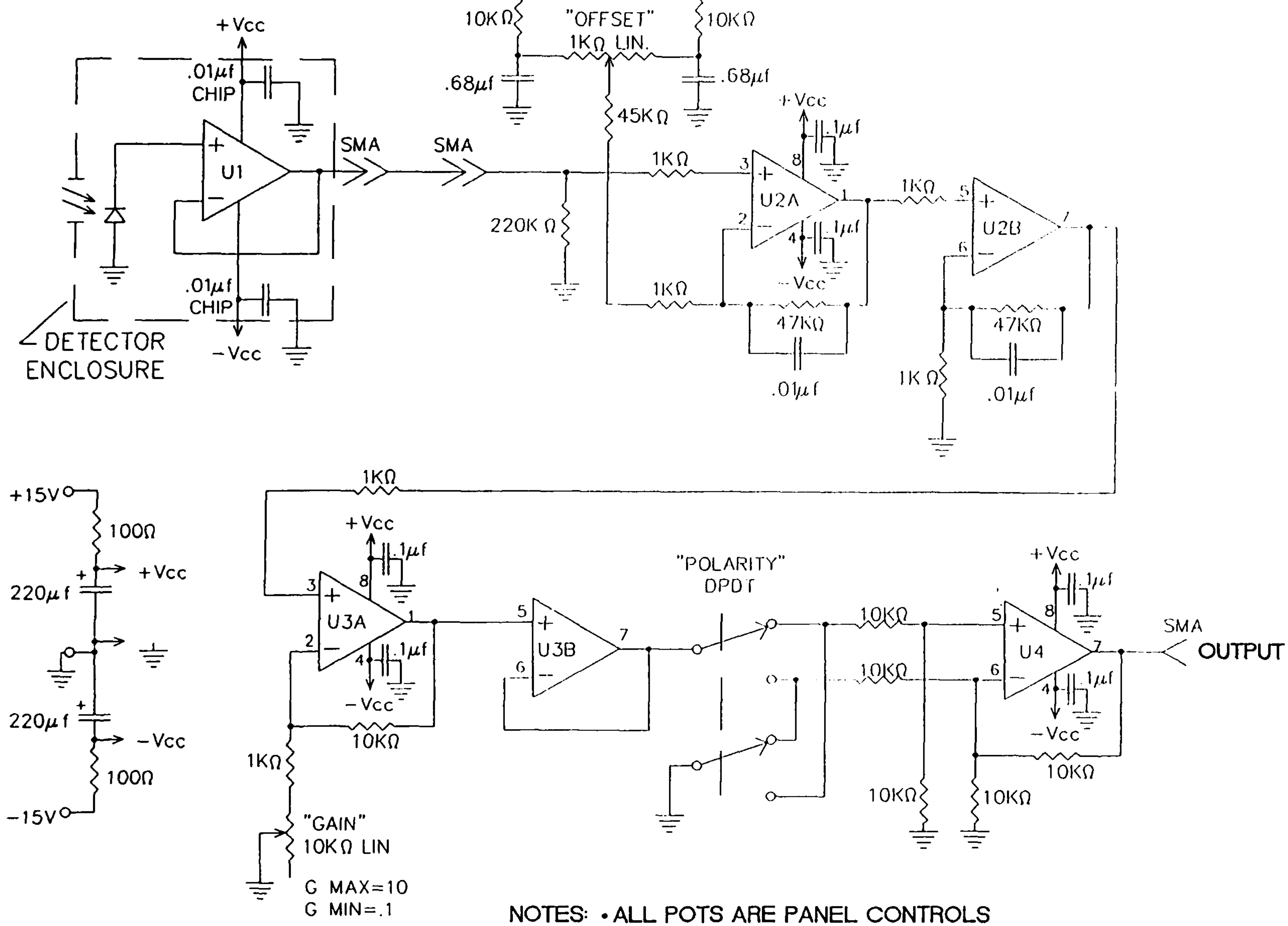

NOTES:
- ALL POTS ARE PANEL CONTROLS
- ALL CAPS IN µf
- ALL RESISTORS IN OHMS
- UI = OP-27, U2-4 = 5532

VISBLDET.DWG

Figure 3

Figure 4 shows the target scene before the image was taken. Figure 5 shows the visible LADAR image. The image is not reproduced very well in the picture shown, however, careful inspection shows that the majority of the objects in the scene can be identified from the image. This image was taken with a DC lighting source being used, not the 60 Hz laboratory lights. The main problem that was encountered in the visible channel was the presence of 60 Hz indoor lighting noise in the images that were taken. This was caused by the fluorescent lighting in the laboratory reflecting off of the target scene and into the detector. This problem was overcome by using a DC lighting source with the lab lights turned off. In the spaceborne solar illumination scenario, 60 Hz lighting noise would not be present.

Along with the visible video channel implementation, a quick-look range processor was also added. Prior to the beginning of this project it was expected that we would have a fully operational high speed digital range processor already installed under our current NASA Phase II program. This program was delayed in starting by 5 months causing us to utilize a quick-look AM-CW range processor constructed to test our NASA Phase II modulators. Our approach used an AM modulation frequency of 100 MHz providing a 30 inch unambiguous range, due to the π phase sensitive detector.

The transmitter optical modulation implementation consisted of a standing wave, Germanium acousto-optic modulator, IntraAction Corp. Model SGM-503. This modulator, when driven with an RF signal of 50 MHz, amplitude modulates the 10 micron optical carrier at twice the drive frequency, or 100 MHz. Additionally, this carrier is then frequency upshifted by a second acousto-optic modulator. This travelling wave modulator, InterAction Corp. model AGM-1103, upshifts the optical carrier and sidebands by 110 MHz. The resultant heterodyne return RF spectrum will have a carrier at 110 MHz, and lower and upper sidebands about the carrier at 10 MHz and 210 MHz respectively. The upshifted carrier frequency is used to eliminate baseband foldover of the sidebands, and to yield directional Doppler when imaging moving targets. The beam size and divergence was not optimized for 2 modulators at 100 MHz.

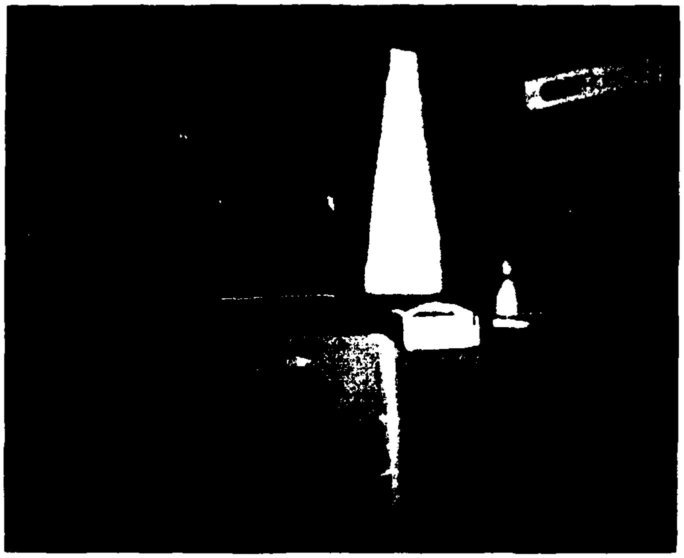

Figure 4. Target Scene

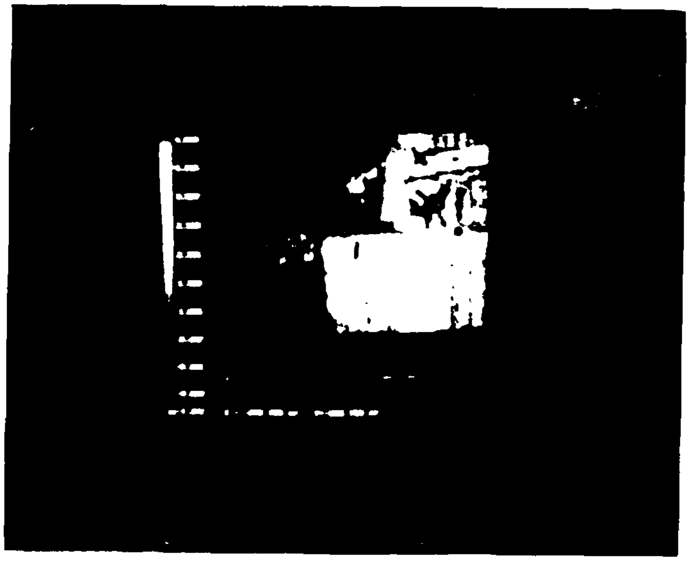

Figure 5. Visible LADAR Image

The receiver approach used was a sideband analog implementation. Referring to the processor block diagram in Figure 6, the received carrier and sidebands were amplified, filtered, and down converted to baseband by a filtered version of the carrier. This baseband signal was then filtered, amplified and compared against a sample of the transmitted modulation in a phase sensitive detector (PSD). The DC output of the PSD is low pass filtered and outputs a DC voltage proportional to the phase difference of the received and transmitted waveforms which is proportional to the range. A graph of the data taken is shown in Figure 7. This data was taken using a linear translation stage with a retro-reflector atached as the target. The target was incremented in one inch steps. The range was measured, at each point, yielding the graph shown and showing a 30 inch unambiguous range. This wideband analog approach suffered from three distinct problems that will be totally eliminated in the Phase II design. The first problem was narrowband CW interference at 75 MHz from the waveguide laser RF power supply, 50 MHz interference from the AM modulator driver, and narrowband interference at 150 and 220 MHz from the third harmonic of the AM modulator driver and second harmonic of the frequency shift AO driver, respectively.

The second problem inherent in the wideband design was the 300 MHz front end noise bandwidth of the system. As ATC is continuing to strive for advanced innovative solutions, the Phase II approach will utilize complex digital state-of-the-art FFT processing. In the coarse acquisition mode, and a 20 MHz acquisition bandwidth, a 1024 point complex FFT will have 20 kHz bins; and in the fine 330 kHz tracking mode, a 1024 point transform will have 330 Hz bins. The CNR improvement over the Phase I 300 MHz approach will be 10 log $(300\text{x}10^6/20\text{x}10^4) \approx 40$ dB for the coarse mode, and 10 log $(300\text{x}10^6/330) \approx 60$ dB for the fine track mode. This Phase II CNR improvement represents a substantial performance improvement over the Phase I implementation.

The third problem encountered in Phase I was an amplitude dependant range measurement. This was due to the fact that no automatic gain control (AGC), capability was used in the Phase I breadboard. The Phase II approach will utilize an FFT phase measurement approach and therefore will be fundamentally not amplitude coupled.

RANGE PROCESSOR—RF SECTION BLOCK DIAGRAM

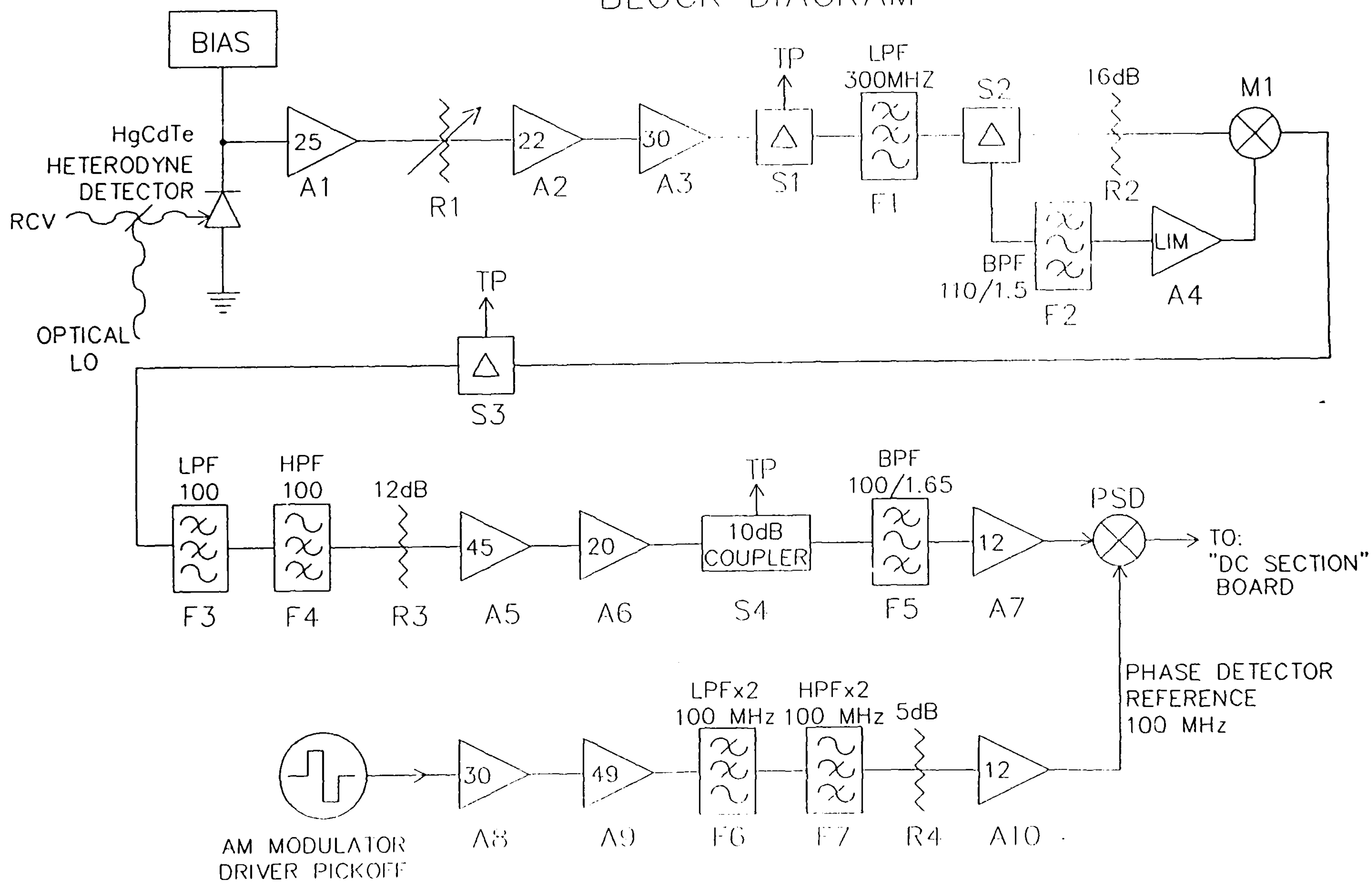

Figure 6

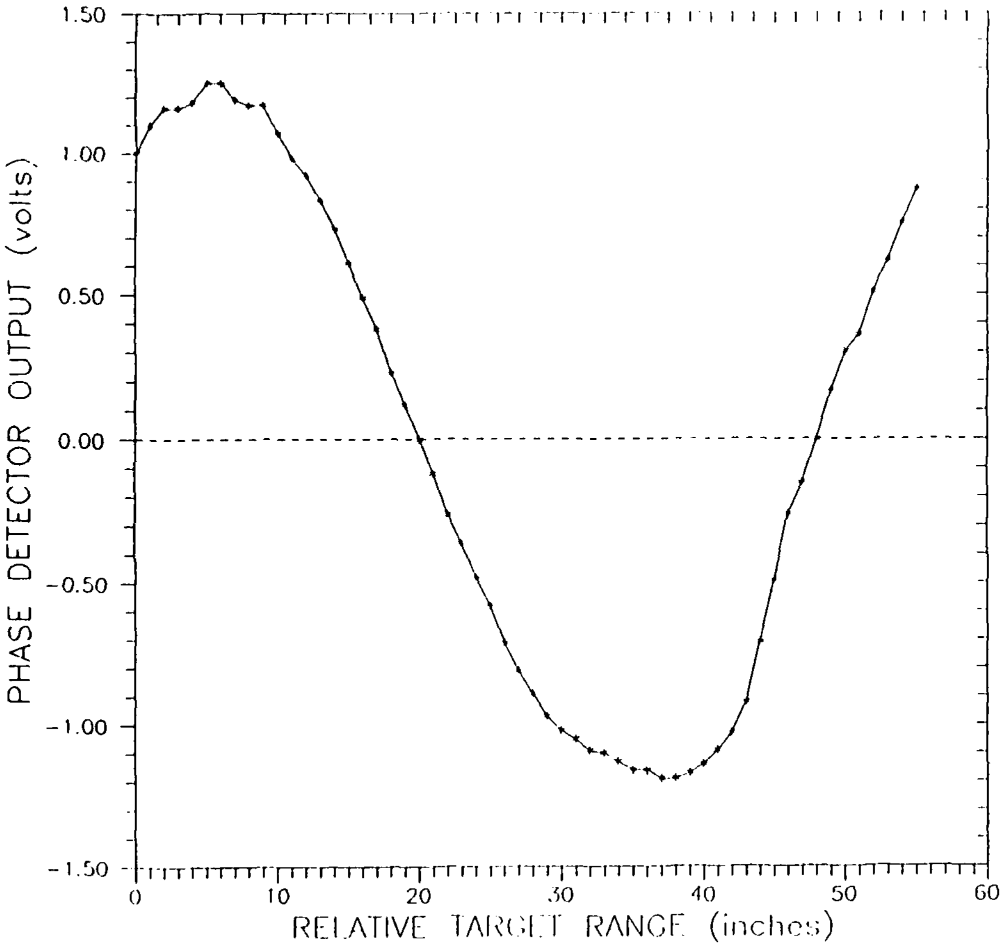

PHASE I ADAPTIVE GRASPING AM-CW RANGE PROCESSOR TRANSFER FUNCTION SHOWING 30 INCH UNAMBIGUOUS RANGE MEASUREMENT RETURN FROM 1 INCH RETROREFLECTOR

Figure 7

III. POSE MATCHING SOFTWARE

The second task to be performed was the coding of the vector points algorithm for adaptive grasping and the range image correlation algorithm. Before the vector points algorithm could be coded, two problems had to be solved. The GMF robot had to be programmed via its KAREL Operating System to accept commands over its C3 external RS232 port. Once a resident KAREL program was installed and operating on the GMF robot, other programs could be uploaded and executed. Secondly, a coordinate system had to be defined for the entire system, including the LADAR sensor. It was decided that the origin (0, 0, 0) of the coordinate system would be the front surface of the LADAR HEAD. From this determination the robots world, user, and tool coordinate systems were calculated. Once these parameters were tied down, the vector points algorithm was coded. When executed, the program prompts the user for the range, azimuth, and elevation for the defined points on both the end effector and target. Those points are G1, G2, G3, and G4 for the end effector and T1 and T2 for the target. The defined locations of these points are shown in Figure 8. Once these points are input, the program calculates the centroids, location, and orientations of the target and grasper with respect to the origin of the coordinate system which is the LADAR HEAD. Given this data, the program then calculates the movement commands given to the robot and sends them to the robot controller whose resident program then executes them. The grasper move to the target is performed in 3 steps. First, the orientation difference between the two is nulled out. Next, the grasper moves to the approach vector, defined by the target, and then finally moves in for the grasp along the approach vector. Another mode of operation that was programmed in provides for manual relative and absolute moves via keyboard command (position) input. This is useful for calibrating and checking the defined coordinate systems.

Figure 8. Grasper Target Orientation

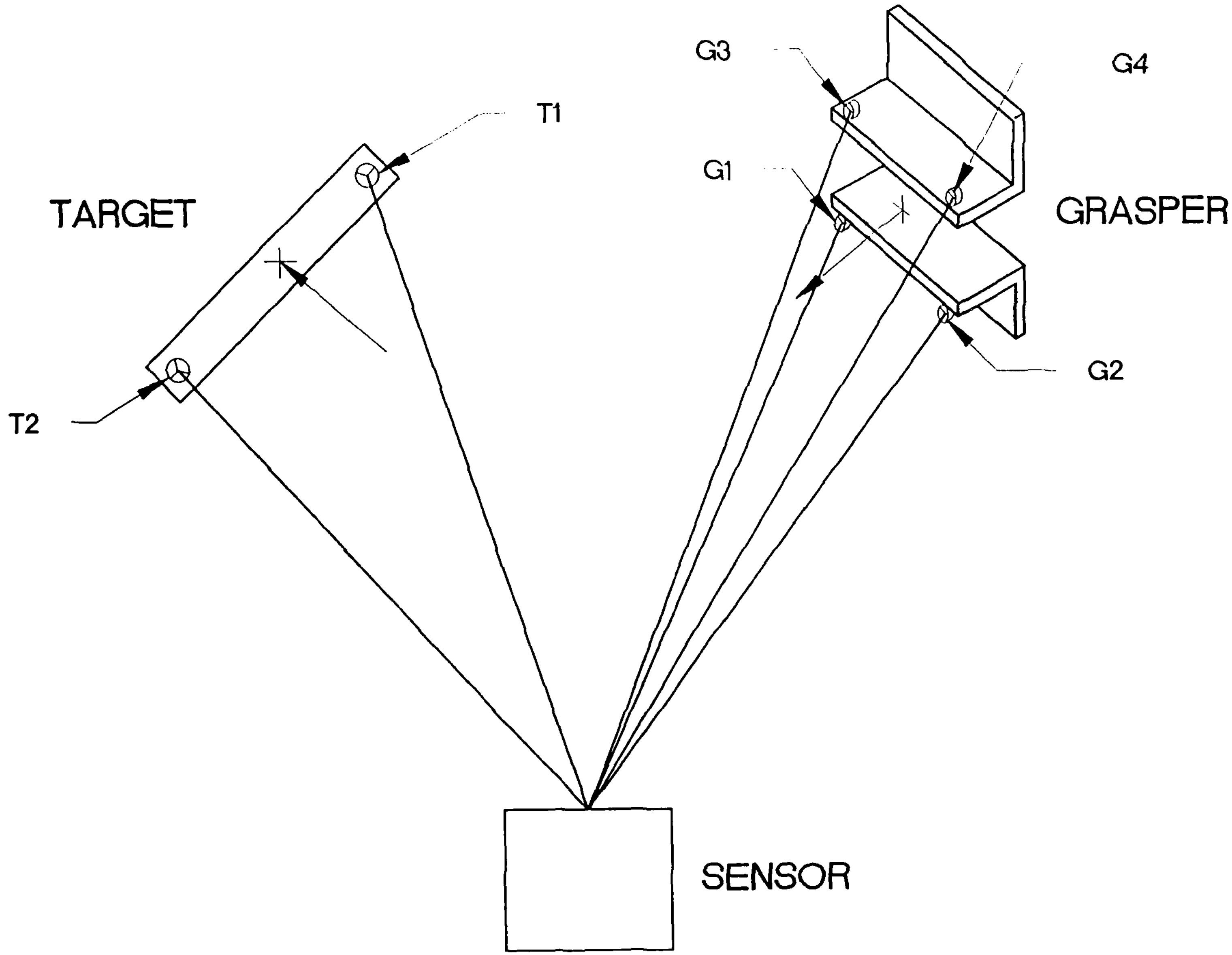

The range image correlation algorithm was coded next in the C programming language. This software was designed to take as input a range image, generated by the ATC LADAR, and a CAD reference image. Once input, a 2D FFT is performed on each of the images separately. This is done by implementing a series of one dimensional FFT's on each of the rows or columns of the image using the separability property of the 2D FFT. Once each of the images has been transformed, the real (LADAR) image and the reference image are multiplied together. This product of the two image transforms is then inverse-transformed yielding the 2D correlation function. The main problem encountered here was the difficulty in converting the LADAR range images into a format usable by the software. The conversion of these images caused the correlation process to be extremely time consuming. This will be solved in Phase II by the use of a dedicated high speed correlation processor. One specific problem uncovered regarding the correlation algorithm, is the tendency of the correlator curve to be flat in the vicinity of the match. The Phase II program will therefore study algorithm techniques to create a sensitive zero crossing function near match. One such approach is similar to a monopulse tracker differencing technique that is very sensitive to small attitude changes.

IV. ROBOTIC DEMONSTRATION

The Adaptive Grasper 3D Correlation Demo system demonstrates the algorithms to be used in the vision processor to identify and register objects detected by the laser ranging system. A secondary function of the demo is to show the nature of the graphical user interface provided by the MacIntosh Computer front end to the system. The demo exists in two parts, the first is a control and information program that allows the user to browse through various high-level schematic diagrams of the LADAR system. This control program yields access to the Adaptive Grasper Simulator which is the control screen for the 3D Correlation Demo. Control Screen in the context of this report refers to graphical images on the computer monitor that have areas sensitive to mouse activation both for software activated switches and text input from the keyboard. A screen capture of a typical Simulator control screen is shown in Fig. 9.

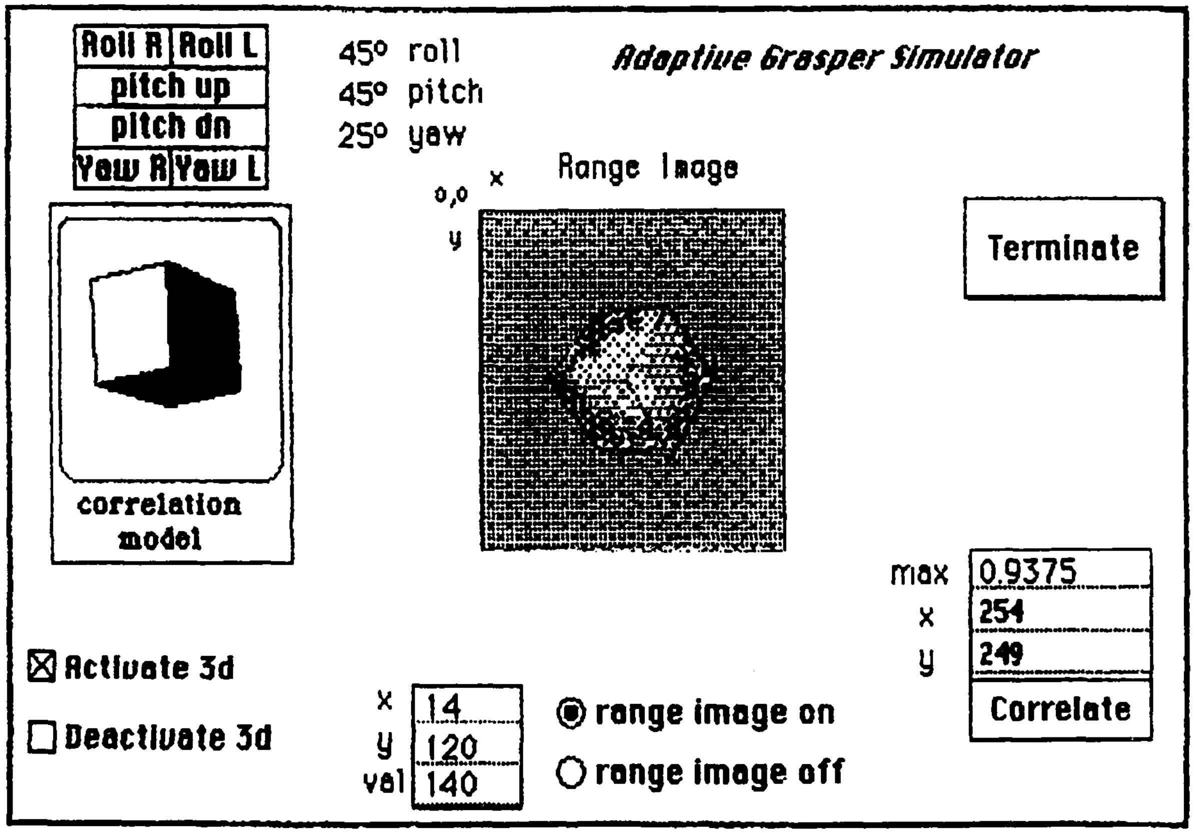

FIGURE 9 SIMULATOR CONTROL SCREEN

The basic algorithm used is correlation. Correlation is determined in three dimensions between a stored model and the range data provided by the LADAR. In the vision processor, the stored model will be constructed dynamically from parameters determined from the operator and key features resolved from all data available to the system. The most important of these parameters are object identification and centroid distance to the object. Identification tells the system which model to retrieve from the database and centroid distance determines scaling. Identification can be supplied by the operator or an algorithm can be applied. Centroid distance can be estimated from the identification of the object and the mean of the laser range image. The simulation uses only one object, hence identification and centroid distance are known. The control screen shows the current 3D aspect of the internal model as a 2D perspective drawing in a window labelled **correlation model.** This graphic appears when the check box **Activate 3D** is selected by the user. Above the graphic is a set of buttons that are activated by mouse clicks for adjusting the aspect of the model in roll, pitch, and yaw. On the right side of these switches is a readout of the current values in degrees. The model aspect changes dynamically when the buttons are selected and the graphic moves accordingly. Internal values for the graphic are stored for later use by the image generation process. The image generation process is invoked by the correlation function, which is shown in Figure 10 below.

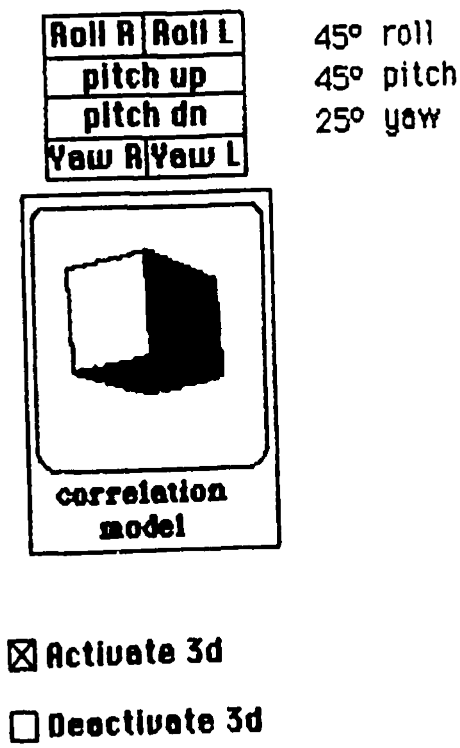

The range image shown in the center of the screen is simulated and the window shows what the LADAR would be seeing, with bright areas indicating closeness and dark representing distance. In Figure 11, the coordinate window below the image yeilds the (scaled to 0-255) range value and coordinates of a mouse selected point on the image.

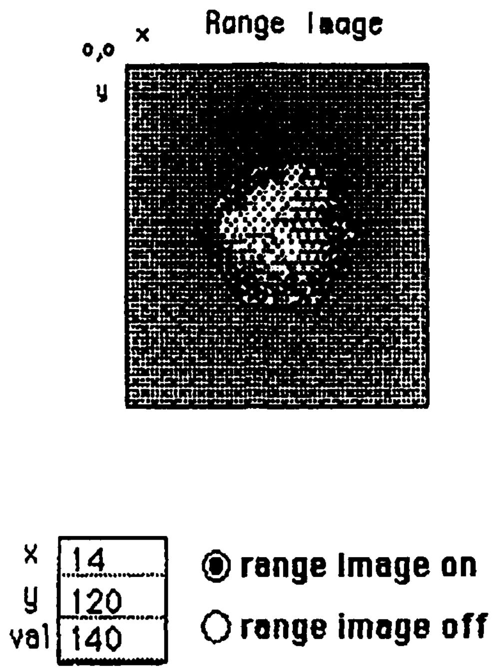

FIGURE 11

The correlation window at the right of the control screen shows the current coordinates of highest correlation (the maximum normalized correlation coefficient) between a synthetic range representation of the stored cube model and the LADAR range image of the cuber. Correlation occurs when the user clicks the mouse on the **Correlate button.**

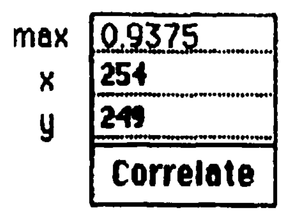

FIGURE 12

When **Correlate** has been selected, a range model representation is calculated from the 3D aspect selected by the user using the current values of roll, pitch and yaw. This data is processed assuming a constant viewer distance that is identical to that used for the synthetic range image. Well known graphic image generation techniques are used on a reference cube to determine normalized viewer distance to non-occluded surfaces. A simple hidden-line removal algorithm provides these surfaces from the user specified aspect angles.

A 2D Fourier Transform is then applied to both the range model and the synthetic range image. The dot product of the 2D transforms is taken and the Inverse Fourier is applied to the result yielding the correlation. The values of the correlation matrix are normalized and the maximum value and its coordinates are then displayed in the window. Fourier techniques are used as the final hardware for the vision processor will incorporate a dedicated Fast Fourier Digital Signal Processor.

All calculations are performed by the host, which in this case is a Motorola 68030 based MacIntosh computer running at 15 MHz. A correlation at a particular aspect angle set takes approximately two minutes. The model is manipulated until the correlation coefficient is maximized. At this point the model and the image will have an identical aspect indicating that the system has locked onto the 3D target. In the vision processor, this activity will be performed automatically with the initial aspect determined from features such as height to width ratio, circularity, and elliptical fit, etc. as shown in Figure 13 on the next page.

These features give clues as to what aspect to begin the correlation. Adjustments to correlation will be performed at real-time speeds. In the simulation this was not possible, hence the reason for the user adjustable model. The slow processing restricted the demo to simply showing the method and algorithm. The demo shows feasibility of the concept by allowing experimentation with the aspect generating and correlation algorithms.

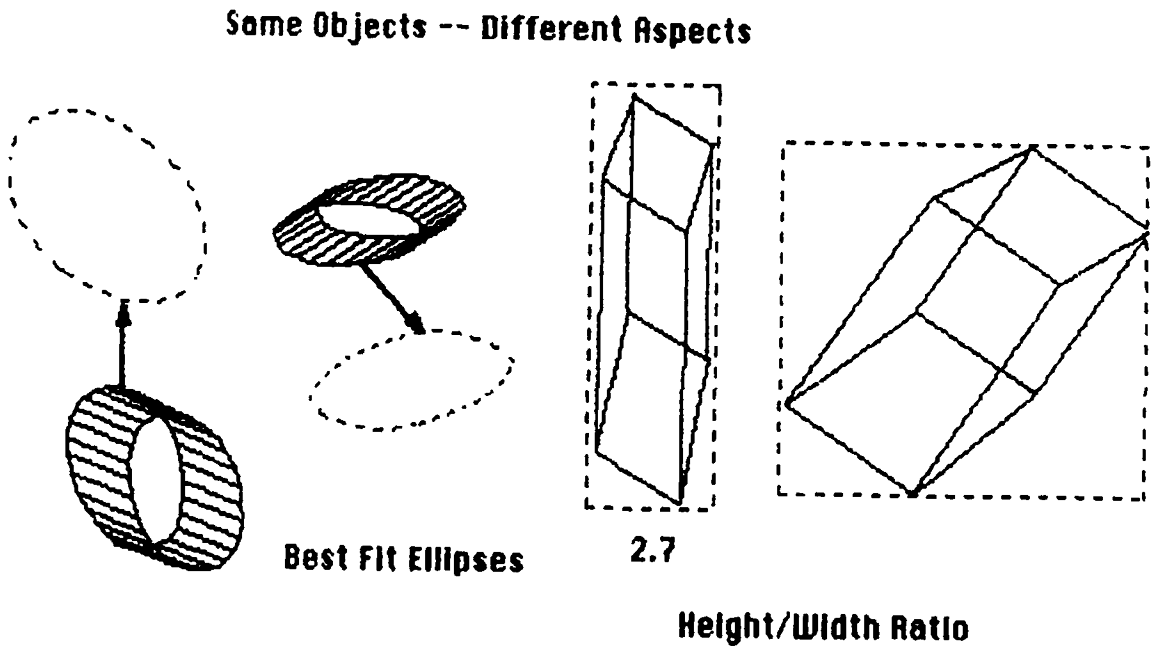
Same Objects -- Different Aspects
Best Fit Ellipses
2.7
Height/Width Ratio

FIGURE 13

The next task of this program was to develop a robotic demonstration to test the concepts implemented. Given that ATC had limited experience in the field of robotics, we subcontracted to Honeybee Robotics (N.Y.), to assist in the robotic systems analysis of this project and potential spaceborne applications. During the analysis it was determined that a "toy" robot, as originally proposed, could not be used due to its lack of position accuracy and weak coordinate system transformation capabilities. Honeybee at this point loaned us an industrial robot manufactured by GMF Robotics. This was a GMF S-100 six axis robot. Once this was decided, a trip was made to Honeybee in New York to learn about the robot's operation and to prepare for its shipping. To accommodate the robot, we added new laboratory space in which we modified the concrete slab with imbedded bolts for the robot to attach to. Additionally, this robot required 208 V line-to-line 3 phase power which had to be added to the lab. Once the robot arrived, it was seated on its mount and powered up for testing where it was found to be operational.

The next problem with the robot was to devise a way to close its pneumatic gripper. This was accomplished by using an air compressor and an electrical pressure switch. This switch was wired to the robot controller's output module on output port number 2. This port is controlled by the controller by assigning an on or off value to the address of the port. Once the robot was mechanically operational, the programming aspect of the problem began to be worked.

The first programming task was to write a communications program on the KAREL System Controller. The program, written in KAREL, utilized the C3 RS232 port of the controller as the input for commands to the robot. It was written and stored in the controller and executed prior to any communications between the robot controller and the PC, which ran the vector points algorithm. Once the communication paths and protocols were established, the coordinate systems for the entire system were defined. It was determined that the front surface of the LADAR head would be the origin, (0,0,0), of the system. From there, the world, user, and tool coordinate systems were derived. Given the coordinate system, the first algorithm to be coded was the relative and absolute move commands. From these programs, the user is prompted to input an X, Y, Z, roll, pitch, yaw coordinate set and the robot would either move to that absolute position, or move that relative increment, whichever was chosen. The second algorithm was the vector points algorithm which is explained in section 2.

As the system was set up, the first thing to be done in a typical demonstration was to power up the robot and execute its calibration routine. Then, the communications program was run, on the robot controller, followed by the vector points algorithm. As input to the vector points routine, the azimuth, elevation, and range of each point, G1, G2, G3, G4 for the gripper, and T1 and T2 for the target needed to be measured. Once these points were input, the robot would execute the grasp of the target in 3 steps, shown in Figures 14 through 17. Figure 14, shows the original locations of the gripper and the target, from which the gripper points and target points are measured. Figure 15, shows the gripper nulling out the orientation difference between the two. Figure 16, shows the gripper moving to position itself along the approach vector to the target and Figure 17, shows the gripper closing on the target ready for a grasp. The end-to-end demonstration was witnessed by Dr. John Johnson, of SDC, who placed the target in a quasi-arbitrary position prior to grasp. Due to the limitation of no path planning software in the robot, the target had to be confined to a range of locations in which it could be placed and expect a successful grasp. If the target was placed outside of this range, the robot would overextend on one of its axis and the program would terminate. This is not expected to be a problem in the future as a spaceborne application would contain path planning software to keep the robot limits from being exceeded. With the placement limitation on the target, the system was able to adaptively grasp the target successfully anywhere inside the limits.

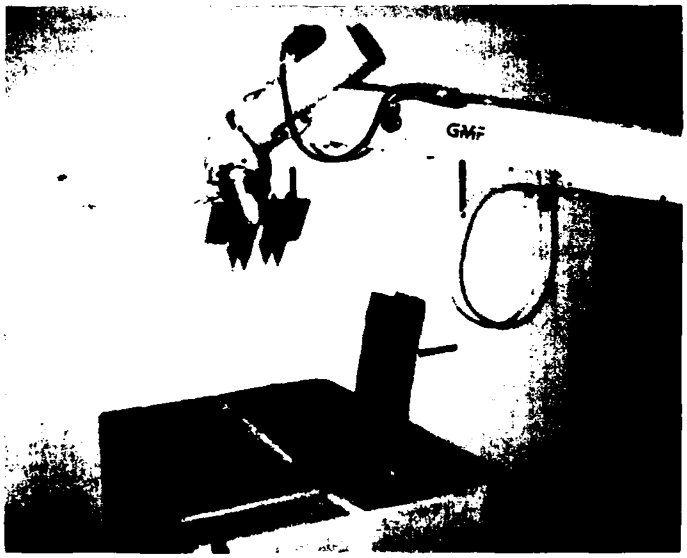

Figure 14

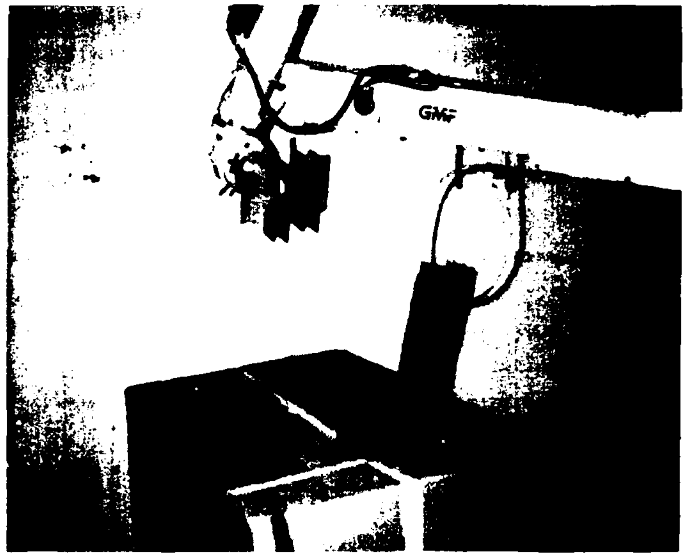

Figure 15

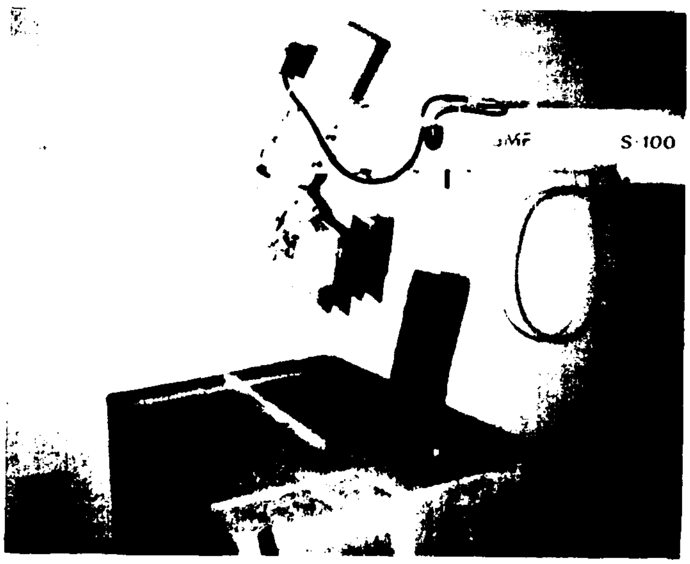

Figure 16

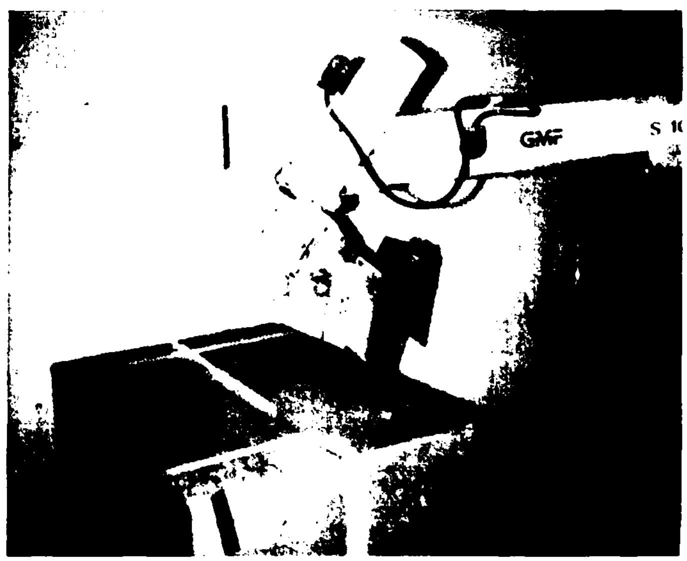

Figure 17

V. PHASE II TECHNICAL APPROACH

The fourth and final task of this project was to explore a concept definition for a Phase II program. To gather information on this several trips were made to meet with the SDIO SSSFD Program Managers and Engineers as well as the NASA SSSFD Program Manager and Robotics and Vision Engineers. The concept definition that follows includes contributions from our key consultants in the fields of Computer Architecture, Fourier Domain Processing, Geometric Data Processing, and Hardware/Software implementation. Given their input, requirements were added for rendezvous and docking because of the technical similarity of the problem (6 DOF Tracking).

1) Imaging LADAR Systems Concept for Autonomous Satellite Servicing

The simplified description of our treatment of both the rendezvous/docking problem and the grasping/manipulator problem is as follows:

Rendezvous and Docking

When the 3D image correlation tracker loop is closed, the 3 space orientation and perspective scale (3 space position) of the reference that maximizes the correlation result will form a high signal-to-noise ratio measure of the 6DOF position of the target with respect to the platform fixed LADAR. These 6DOF error signals of the target with respect to the platform, along with their rates, will allow the G & C computer to optimally calculate propulsion commands to perform rendezvous & docking. This concept is shown in Figure 18.

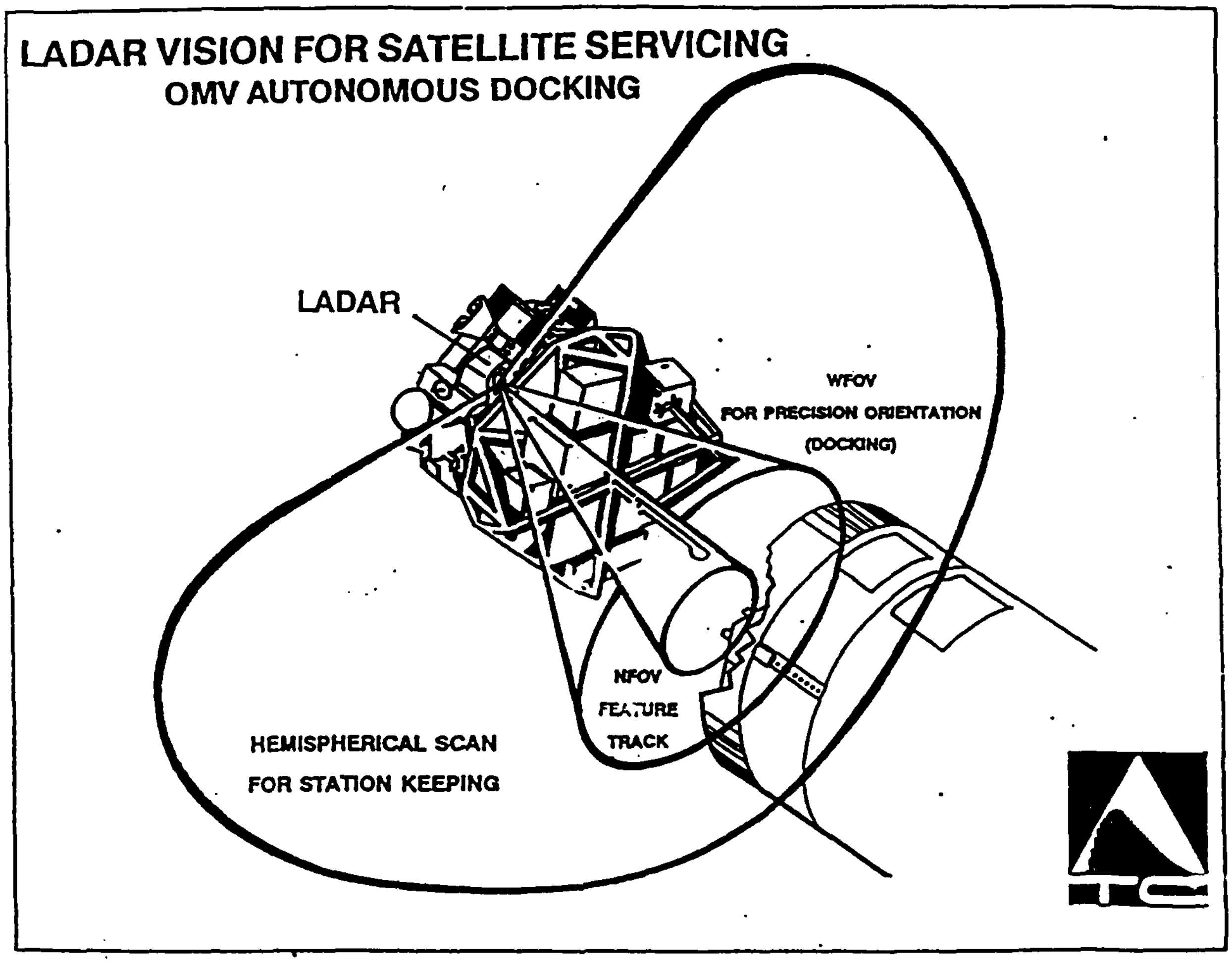
LADAR VISION FOR SATELLITE SERVICING
OMV AUTONOMOUS DOCKING
LADAR
WFOV
FOR PRECISION ORIENTATION
(DOCKING)
NFOV
FEATURE
TRACK
HEMISPHERICAL SCAN
FOR STATION KEEPING

FIGURE 18

Grasping and Manipulation

The approach is to treat both the actual target and end-effector as targets. Therefore, we are required to view both within the LADAR FOV and thus the process is reduced to performing the 6DOF error signal generation for both target and grasper individually. The robot commands can now be simply calculated as the relative error (in 6 space) of the target with respect to (differenced from) the grasper. This approach attempts to mimic the human where vision feedback is used regularly to pick up objects by first looking at the object (i.e. pen on cluttered desk), then begin moving your arm and hand generally toward the pen until both hand and pen are in your vision. Because your brain has solved the guidance, you can look away and still grab the pen.

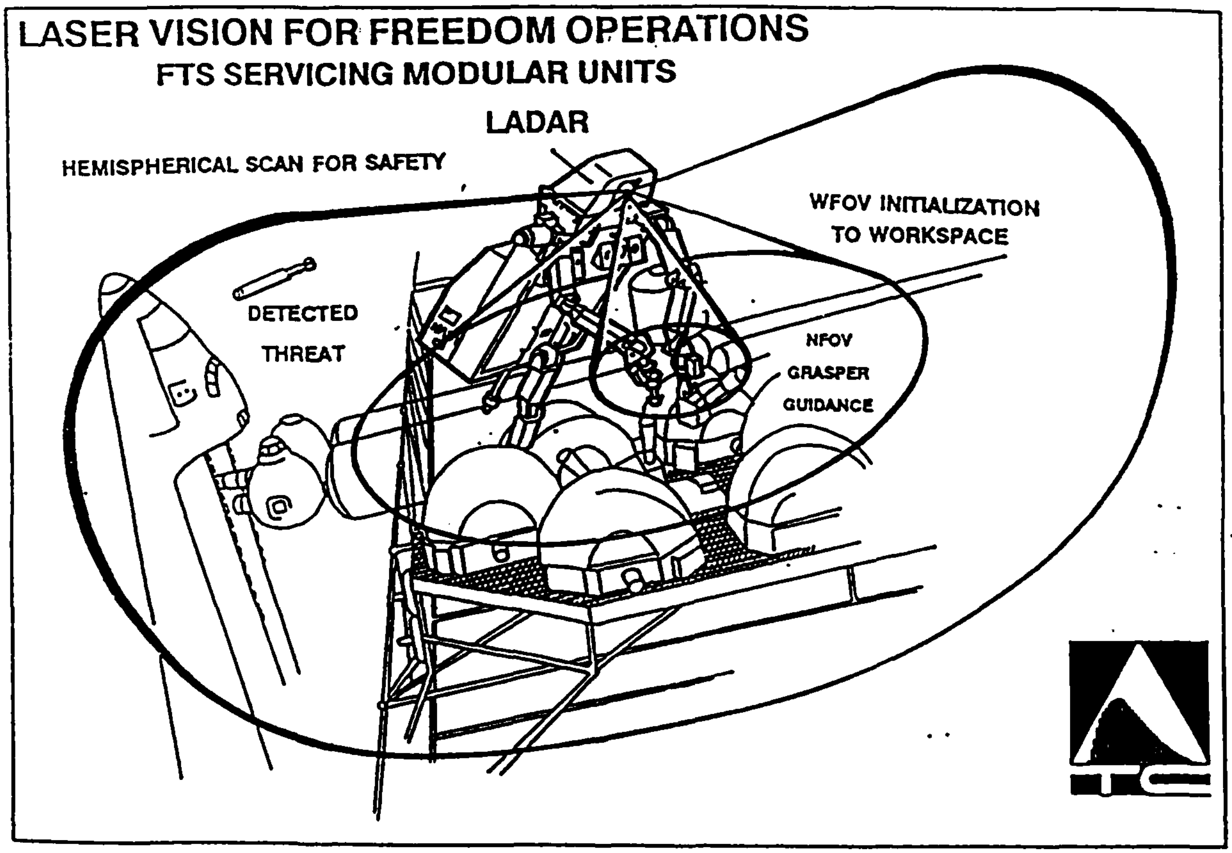

Figure 19

2) Logical Flow of Nominal Systems Scenario

The following narrative is a discussion of a combination of systems, algorithms, and hardware issues with respect to defining some nominal system scenario from which to examine the detailed algorithm and hardware requirements.

<u>Handover/Acquisition of Target Body Based on Spatial Discrimination</u>

Figure 20 is a flow diagram of the logic of the proposed scenario. It begins with the handover to the LADAR System of the identity and approximate location of the target, minus the object to rendezvous and dock with, or to be grasped/manipulated. The handover location need not be precise, but must be sufficiently definitive to identify the object uniquely; i.e., the given location must be closer to the true object than to any other, or additional distinguishing characterizers provided. The coordinate system used in the handover is TBD, but either the sender or the LVP will convert this to a range/angles (i.e., polar) reference, so that it can point the LADAR sensor to the handover location, where it can initiate a search.

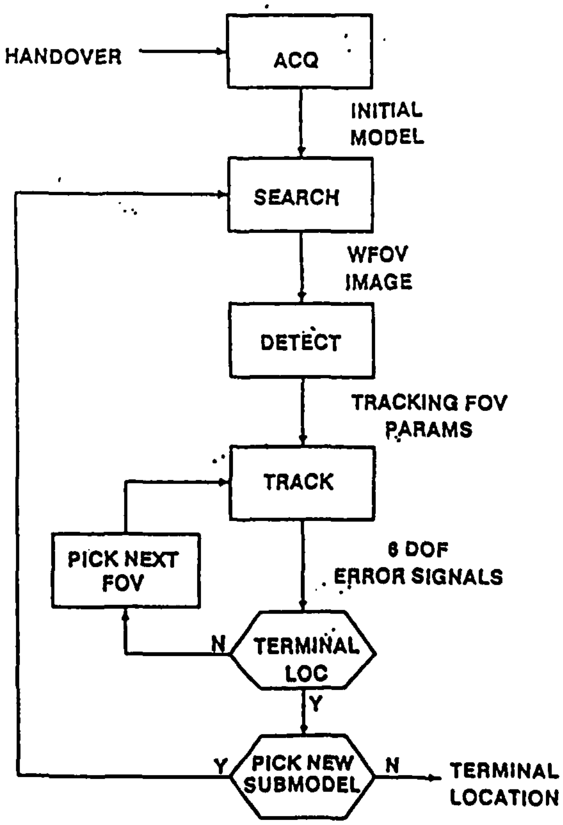

Figure 20

The handover in the form of a state vector predictor when processed, will specify a search volume, from which spreads in azimuth, elevation, and range can be determined as shown in Figure 21. Since the LADAR sensor is collimated to a small instantaneous beam, and yields radial range and velocity as well as reflected intensity and visible video, the sensor defines a small instantaneous sensing volume in a known direction. Searching is effected by sweeping this instantaneous direction in a raster pattern while simultaneously recording the multi-dimensional data. Only range and velocity data associated with all responses above a selected intensity threshold are deemed valid.

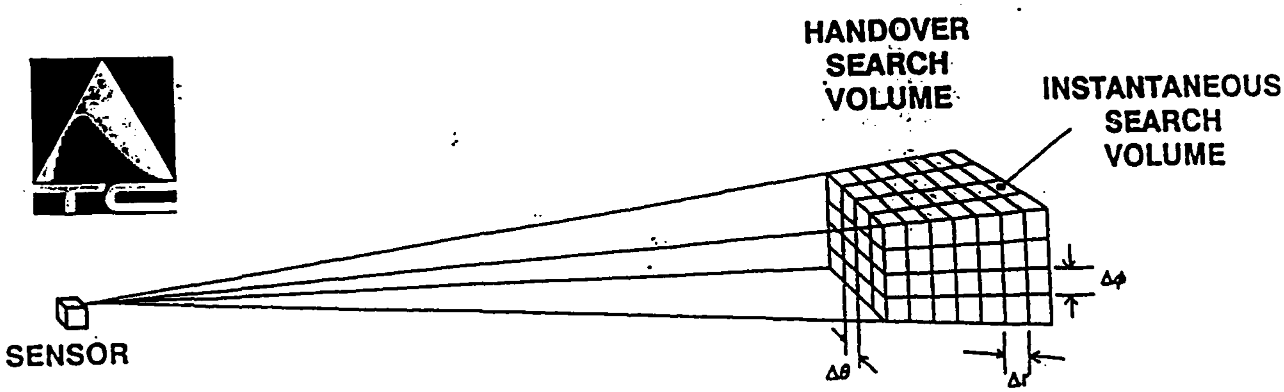

FIGURE 21

The acquisition block in Figure 20 refers to the handover itself, i.e., to the acquisition of the identity and approximate location of the target. The LVP will carry within it, or can have uploaded, the information describing the form factor of the target, details of the docking surface and any constraints on where it may or should not be grasped. Typically, these data will originate in the CAD construction drawings of the target, and will be converted to hierarchal polygon models and hereto will be referred to as the target data base.

<u>Search</u>

At this point, the search begins for the target characteristics that identify its orientation and verify its identity. The rest of this discussion will concentrate on the former with the observation that the processes described will not be successful unless the later holds. That is, the scenario used precludes grasping the wrong object.

The process is cyclic, and at this point we enter the main loop. The search begins with a field of view wide enough to encompass the entire handover volume. In a non-passive sensor such as our LADAR, the FOV (field of view) is actually the scanned field, and does not describe the optical FOV of the receiving optics, with which it could be confused. The result of the entire scan is an image of the space contained within the FOV. Typically, the initial scans will be of mostly empty space, with only a few pixels responding. The target may or may not be resolved, depending on how far away it is, how large, and the sensor resolution. For this discussion, a target is considered resolved if the image (not the optics blur) is larger than a pixel. Unresolved targets may thus activate one to four pixels, depending on how close they are to pixel boundaries and their size.

<u>Detect</u>

In most cases, the acquisition of the target body is accomplished using MTI or moving target indications based on the velocity image of the search FOV. Thus, as soon as the target is detected, a fairly good target direction is available. Since range is observed, the uncertainty in target range is also now small, resulting in a new search volume that is now considerably smaller than the handover volume. Then, subsequent sweeps can be over a smaller

FOV, and for a given number of pixels per scan can be over smaller, possibly overlapping, pixels. Adaptable optics (e.g., zoom lens) will produce actually smaller pixels and improved resolution. As the target is approached, the resolution then improves continually.

Track

As soon as the target is well resolved (which may be at the beginning), the task of the LVP switches from search to that of determining the target's orientation and accurate position. To do this, the on-board computer accesses its target data base. This contains the detailed polygon model of the target. While following the steps described below, the LVP also continually adjusts its FOV (zoom lenses and sweep amplitudes) so that the target size relative to the FOV is near optimum. That is, it continually adjusts its tracking parameters, based on feedback from the most recent images, known rate of closure, changing view requirements, etc.

As it tracks, its behavior is best described with an auxiliary loop, shown in Figure 20. It enters the loop with a postulated orientation of the target in pitch, yaw, and roll, and derives a theoretical image of what it should look like from the target data base. Then, it continually determines whether or not it has adequately matched the postulated orientation and perspective view against the actual view that it can unambiguously decide these parameters known to the required accuracy. If so, it picks a new, generally smaller, FOV and iterates the process as the range closes, thus tracking the target in six degrees of freedom, i.e., orientation as well as position. If it is unable to achieve an adequate match from the postulated surface or feature identification, it picks a new sub-model, that is, a new postulate of the identity of features or surfaces on the observed image. Then it re-enters the outer loop, iterating it again. This time, however, it already has the advantage of tracking information in the three position DOF's, thus facilitating the iteration. The emphasis is now on orientation, and it may pass rapidly through both loops several times as inappropriate models are considered briefly.

Eventually, the process converges to the point where the features of the target are identified unambiguously. From here, the process is one of refining the orientation information. This is still a three-dimensional manifold of unknowns, viz., relative pitch, yaw, and roll, and all change with closure. At each attempt to form a match of theory to observation, a considerable amount of logic and "number crunching" is involved. The process is one of area correlation. The observed pixels of any opaque image form a surface, and in the same manner used in image simulators, the subset of area elements which is observable from a postulated location can be identified, and the appearance of the (possibly discontinuous) surface they form can be determined. That is, a perspective view from the assumed viewpoint can be formed. This can then be compared with the perspective view obtained from the sensor to make a 2D -or area - correlation. Since range is also available for every pixel, both theoretically and observationally, it can be used for the correlation variable, that is, the quantity compared. In effect then, one is matching two space surfaces for best geometrical fit. To get a good fit, the model must have accurate values of postulated roll, pitch, and yaw, thus determining the target orientation when a good fit is obtained. The mathematical process of making the fit is that of use of the two-dimensional Fourier transform. The basis is that the correlation is the inverse transform of the product of the two direct transforms of the two images to be correlated. The DASP chipset, allows extremely fast Fourier transform or inverse transform.

One also has the option of filtering or smoothing the observational data prior to correlation to smooth out random error. Even if the fluctuations are real, filtering can have the effect of giving a more rapid convergence of the iterative fit, by removing the texture correlation until the match is comparable to the amplitude of the texture fluctuations. We propose to develop an adaptive filtering technique that uses filtering to the degree appropriate to the case at hand. Techniques to be developed during the program will develop sensitive error signals that will indicate which way to move in which variables to get to the next model 6DOF parameters for making the iterative set of correlations converge rapidly and effectively.

Everything described so far applies equally well to two current servicing problems, viz., those of docking of a servicer platform (OMV) with a large object to be serviced, and of locating the optimum place to grasp a small object (e.g., tool) and maneuvering the manipulator to get in the right position. The adaptive grasping problem has an additional requirement over the docking problem, however. Here, one must not only get in the correct position and orientation and know where to grasp, but one must guide a robot hand or equivalent to the right position and orientation and must correctly time the grasp so that the grasping action does not knock the target away. In practice, this translates to a requirement to monitor both the target and the hand simultaneously, and use the closing differences as error signals to make the grasp gentle, positive, reliable, and rapid. Although this doubles the computational load near closing, it really adds little to the system requirements. As with a corresponding human action, the system merely slows down when the task becomes delicate, as it should. Thus the system described here is the solution to two problems, rather than one.

3) Long Range Rendezvous

Recently a 100 nmi requirement became important for a rendezvous sensor that could meet a wide variety of program requirements. This system requirement would be met by the same nominal 2 watt, 1 inch aperature LADAR sensor that has been described as performing the skin target imaging out to 3000 feet. A 3.3 inch retro-reflector on the target would provide 25 dB carrier-to-noise ratio (CNR) at a range for 100 nmi (180 km) using a noise bandwidth of 2.5 kHz. The nominal search of an 8 x 2 x 2 nmi uncertainty ellipse resulting in an approximate angle of 60 x 20 mrad could be searched in 5 seconds using a 0.5 mrad beam at a 1 kHz pixel rate. The processor for this application would utilize a Doppler acquisition center frequency and bandwidth based on the radial velocity prediction and corresponding uncertainty given the state vector handoff. The initial estimate of range would drive the scan rate to not violate the time-of-flight dependant lag angle scan rate limit (equivalent to a pulsed system's range ambiguity PRF limit). After detection, this long range unresolved retro-reflector target would be the ideal target to track in a relatively high frame rate mini image tracker, say 3 x 3 pixels at 1 kHz pixel rate for a 100 Hz tracker.

4) Visible Video Assisted Handover for Large Complex Scenes

The registered visible video channel within the LADAR is a key feature of our LADAR vision approach that can be exploited early in the development of autonomous operations. During tasks involving complex scenes and those where targets and target like objects occupy a common densely packed area, operator assisted acquisition may occur as follows:

A wide field of view TV camera image of the complex scene is displayed to the operator. Utilizing the most advanced vision processor available today (the brain), the operator finds the specific target and identifies it to the LADAR by pulling a window on the display screen that closely surrounds the target, and has the target intersecting crosshairs in the window. The LADAR will derive it's scan FOV from the angular position and subtense of the displayed window. The LADAR can then perform a visible image correlation track between the visible LADAR channel and the WFOV TV camera. The resulting visible image correlation track will allow accurate handover to the registered 3D correlation tracker using the CAD derived orientation specific range image reference. From then on, the LADAR will perform automatic tracking to ease operator workload based on initial manual designation.

5) Acquisition of an Object Among Other Objects Within the Handover Volume i.e. (The Recognition Problem) as an Extension to the Orientation Search Problem

Our basic approach to the recognition and orientation search problem is a modification of the brute force approach that would simply correlate all known objects that could be within the handover volume at all possible orientations each. Correlations could occur until a threshold was crossed or by picking the peak value after all targets/orientations were tested.

Our modified approach solves the problem of the enormous database of image orientations by storing the target CAD based polygon model and doing the image generation on line. Our modified approach will also greatly reduce the number of orientations searched by employing two unique features, a hierarchal target model and a multiple target correlation reference. This method would utilize course, low fidelity models initially that based on a low polygon count per model would allow many targets and orientation to be correlated simultaneously in the following manner:

Consider a 512 x 512 pixel correlation reference made up of 16 separate, 128 x 128 pixel images arranged in an 4 by 4 pattern. A single data frame of 128 x 128 course resolution LADAR image could be correlated against the 512 x 512 composite. Thereby a search of 16 conditions (targets and/or orientations) could be accomplished with a single correlation. The following discussion represents the capability of the proposed processor to search in orientation and/or target space.

To begin this discussion, we must state that we have chosen to optimize our hardware processor for the precision tracking function. This is based on the fact that the near term applications such as SSSFD, will tend to be more constrained, limited domain problems. Recognition and arbitrary target orientations will not likely be the focus of these demonstrations, but rather the demonstration of simple rendezvous and docking and supervised servicing tasks such as fluid transfer and ORU exchange. However, the fundamental nature of this program is to provide a growth path to a more highly generalized and increased level of autonomy.

For a 512 x 512 high resolution tracking image, full frame correlations are accomplished using our proposed architecture at a 15 Hz rate (FFT board rate). We are therefore matched to our baseline reference generator specified at 20 k polygons per sec peak. For a 512 x 512 image, 500 polygon objects represent a very high resolution rendering. The image generator could handle approximately 150% overhead, or an average polygon rate of 8000 per second and still maintain 15 Hz correlation rate and thus a 15 Hz system error signal rate.

Let's consider a relatively stressing initial orientation/search case example whereby we perform a hierarchal search of the entire 4 π hemispherical uncertainty initially at increments of 45° thereby having 360°/45° = 8 views from each of 3 axis or 512 views totally for each target.

Using an approach whereby 256, 32 x 32 pixel course references are initially used, 2 frames would be required for each target in course resolution. Since one correlation of 512 x 512 can be performed in a single FFT board at a 15 Hz rate, individual targets can be searched at a 7.5 Hz rate. Since the polygon rate is fixed at 20 k/sec, which is 1333/15 Hz frame time, there can only be 5 polygons per each of the 256 course references which would represent only simple parellelepipeds, cylinders, etc.

Consider now one scenario for a hierarchal search approach. The following table represents 8 steps in a hierarchal path. Starting from a totally unknown orientation in all 3 axes, we can achieve a high fidelity full image correlation track to <.3° orientation accuracy. This meets the requirements of the NASA Laser Docking Sensor Flight Experiment Program.

TABLE OF HIERARCHAL SEARCH PARAMETERS

							Search Examples	
Step #	Ref Image Size	# Refs in 512x512 frame	# Polygons Per Ref Real-time	# Image Correlat @15Hz Rate	N Total Views	3 Axis Improvmt $\sqrt[3]{N}$	Initial Unre All Axis	Ending
1	32x32	256	5	2	512	8	360°	45°
2				2			45°	5.6°
3	64x64	64	20	1	64	4	45°	11.25°
4				1			12°	3°
5	128x128	16	83	1	16	2.5	3°	1.2°
6							1.2°	.48°
7	256x256	4	333	2	8	2	.48°	.25°
8	512x512	1	1333	1 Single Image Tracking				

10 Image Correlations Total

Till Track ≈ 1 sec

6) LADAR Vision Imager (LVI) Technical Description

NASA PHASE II LVI, SPECIFICATIONS

Laser Transmitter: 2 Watts RF Excited CO_2 Waveguide Laser
Optical Receiver: Closed Cycle Cooled 77K HgCdTe Heterodyne Detector
Registered Imagery: Range, Velocity, Intensity, Visible Video
Maximum Range: 3000 ft. Skin Targets
100 nmi 3.3 Inch Retro-Reflector
Modulator: RF Driven Ge Acousto-Optical Modulator
Waveform/Processor: 3 Frequency AM (DME): 100 kHz, 2 MHz, 100 MHz Selectable
Range Ambiguity: 5000 ft 250 ft 5 ft
Range Accuracy: 1% @ 20 dB CNR: 50 ft. 2.5 ft .05 ft (.6 in.)
0.1% @ 40 dB CNR: 5 ft. .2 ft .005 ft (.06 in.)

Doppler Processor: 1024 Point Digital FFT w/ SPT DASP/PAC 32 Bit DSP
Acquisition: ± 21 ft/s = 2.5 MHz Bandwidth Range Rate Coverage
±.02 ft/s = 2.5 kHz Resolution for Acquisition
Docking : ± 2 ft/s = 250 kHz Bandwidth 1024 DFT (Same Board)
±.002ft/s = 250 Hz Resolution for Terminal Docking

Optical Transceiver: Monostatic Compact Interferometer .5 in. Aperture
1 inch Output Aperture to Galvo Scanners (El, Az)

Angular Beamwidth: .5 milliradians 90% Power
Foveal Scan NFOV/WFOV: ± 20 Degrees Random Access, 5/1 millisec Step
2.5 millrad (for 5 x 5 Mini-FOV) 1 kHz Sine
Peripheral Scan: Hemispherical Coverage
Pixel Format: 1 Hz to 100 kHz, $(1024)^2$ Programmable
System Controller: Transputer Network (12)

Link Analysis: ATC Carrier-to-Noise Ratio Simulation Output: NFOV, Skin Target

P= 2 Watts	ETA.S= .01 System Effcy	RHO= .02 Diffuse Refl	D= .026m 1 in Dia.	B= 2.5 BW kHz	ALPH= 0 Atmos dB/km	R= 1 km

CNR = 31.60 dB (41 dB in 250 Hz BW)

Prime Power 300 Watts Continuous, 30 Watts in Duty Cycle Mode
Size: 12" x 12" x 12"-Sensor Head, 19" Rack 15" High Phase II LADAR Processor
Weight: 75 lbs 24 VDC Version
Program Information: Delivery to NASA/JSC Phase II LADAR Vision Imager (LVI) - 1 Aug 1990

VI. CONCLUSION

To conclude this report, a summary of the tasks performed and results obtained is given below.

The first objective of the program was to integrate a registered visible channel into the existing ATC LADAR. This task was accomplished successfully with only one minor problem occurring which was 60 Hz AC lighting noise. It was determined that this would not be a factor in a spaceborne scenario and could be handled easily by post detection filtering.

Secondly, we were tasked to create the pose matching software. Several problems had to be overcome, such as coordinate system definition and communications with the KAREL Robotic System Controller, as well as several minor obstacles. These were successfully solved and the vector points software was implemented as planned. The correlation software was generated successfully as well, but its implementation required extensive translations of the images to be used into the proper format which caused extremely inefficient operation. This problem will be solved in the Phase II program by the use of a dedicated high speed processor.

The third task was to demonstrate the concepts implemented in the previous tasks. To facilitate this, a GMF S-100 six axis robot was installed at ATC on the recommendation of our robotics system consultants, Honeybee Robotics. Additional lab space was acquired for the robot and substantial lab upgrades such as a custom concrete slab and three phase power source were implemented for its installation. In addition, there were many small problems that had to be solved prior to the robot's programming and subsequent use. Although many bugs were encountered within the robotic system, the basic concepts of the program were successfully demonstrated.

As the final task of this program, a Phase II concept definition study was performed. It addresses an end-to-end approach for the problem of Real Time demonstration of Rendezvous, Docking, and Grasping.

Overall we are pleased with the results of this program in that the goals set in the Phase I proposal were met successfully. In addition, a Phase II concept definition study was performed which concludes that a Real Time implementation of this innovation is feasible.